Journal Pre-proof

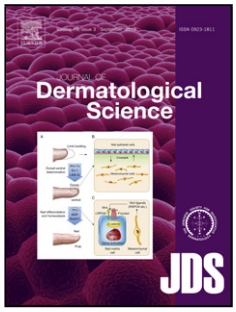

Exogenous pyruvate alleviates UV-induced hyperpigmentation via restraining dendrite outgrowth and Rac1 GTPase activity<!–<ForCover>Choi S-Guk, Kim J-Hyun, Hong S-Heon, Lee OY, Kang N-Gyu, Exogenous pyruvate alleviates UV-induced hyperpigmentation via restraining dendrite outgrowth and Rac1 GTPase activity, *Journal of Dermatological Science*, doi: 10.1016/j.jdermsci.2020.11.006</ForCover>–>

Seon-Guk Choi, Jin-Hyun Kim, Seong-Heon Hong, Oun Young Lee, Nae-Gyu Kang

PII: S0923-1811(20)30355-8

DOI: https://doi.org/10.1016/j.jdermsci.2020.11.006

Reference: DESC 3683

To appear in: *Journal of Dermatological Science*

Received Date: 14 February 2020

Revised Date: 5 October 2020

Accepted Date: 10 November 2020

Please cite this article as: { doi: https://doi.org/

Exogenous pyruvate alleviates UV-induced hyperpigmentation via restraining dendrite outgrowth and Rac1 GTPase activity

Seon-Guk Choi*, Jin-Hyun Kim, Seong-Heon Hong, Oun Young Lee and Nae-Gyu Kang

R&D Center of LG Household and Health Care, Ltd., Seoul, 07795, Korea

*Corresponding author at : 70, Magokjungang 10-ro, gangseo-gu, Seoul, 07795, Republic of Korea. Tel. : + 82 10 8770 0069.

E-mail address : csg24@lghnh.com (Seon-Guk Choi).

Highlights

- Exogenous sodium pyruvate displays anti-melanogenic properties.
- Intracellular pyruvate suppresses dendrite elongation by inhibiting Rac1 pathway
- Pyruvate treatment alleviates UV-induced hyperpigmentation in reconstructed human skin equivalent

Abstract

Background : Melanin is synthesized in melanocytes and transferred to keratinocytes through dendrites. Endogenous pyruvate is a key metabolite for ATP production in glycolysis, and the tricarboxylic acid (TCA) cycle and exogenous pyruvate provide protection against oxidative stress and acidosis in the intercellular space. The function of pyruvate in the regulation of dendrite outgrowth remains to be elucidated.

Objective : We examined the effect of pyruvate on dendritic elongation and skin pigmentation

Methods : Murine B16F10 melanoma cells and human primary melanocytes were used for *in*

vitro analysis. Melanin quantitation and histochemical staining were performed in a 3D pigmented human skin model.

Results : We demonstrated the participation of monocarboxylate transporters (MCTs) responsible for the membrane transport of pyruvate in B16F10 melanoma cells. The accumulation of pyruvate occurred in a pH-dependent manner, which was highly sensitive to a specific MCT inhibitor (α-cyano-4-hydroxycinnamic acid). α-MSH-induced morphological changes, including dendrite elongation and growth-cone-like structure, were diminished in B16F10 cells upon treatment with pyruvate. In addition, the number of dendrite branches was reduced in normal human epidermal melanocytes. As the Rho-subfamily of monomeric GTP-binding proteins modulates dendrite formation, we subsequently examined the suppression of Rac1 activation by pyruvate, but not RhoA and Cdc42. Furthermore, pyruvate showed anti-melanogenic effects against UV-induced pigmentation in reconstructed pigmented epidermis, established by co-seeding autologous melanocytes and keratinocytes, which act similar to *in vivo* skin tissue.

Conclusion : These results suggest that pyruvate treatment may be an alternative or additive therapeutic strategy to prevent hyperpigmentation.

Keywords: pyruvate, melanin, dendrite, skin, pigmentation, UV

1. Introduction

Melanin biosynthesis, which is necessary for skin defense against UV radiation and other stimuli, is the major cause of dark skin pigmentation [1]. The initiation and extension of melanogenesis occurs in the melanosome (endosome/late endosome-delineated organelle),

depending on the tyrosinase enzyme (TYR), which catalyzes the initial rate-limiting reaction in melanin biosynthesis, tyrosinase-related protein 1 (TYRP1), and dopachrome tautomerase (DCT or TYRP2). In the skin, melanosomes are transferred from the dendrites of melanocytes to the surrounding keratinocytes through an intricate network of dendrites, in response to hormones and UV radiation [2]. To accomplish efficient melanosome transfer, melanocytes markedly increase the length and number of dendrites, since the melanocytes constitute a minority population in the epidermis and must contact multiple keratinocytes [3]. Previous studies have demonstrated that dendritic outgrowth is enhanced by growth factors and UV radiation [4].

The outgrowth of dendrite tips is promoted by rearrangement of actin filaments and microtubules, and the underlying signaling mechanisms have been investigated [4, 5]. The small Rho-subfamily of GTP-binding proteins orchestrates cell polarity, cell-cell adhesion, vesicle transport, and differentiation through their ability to regulate actin assembly [4]. Like the majority of Rho proteins, they fluctuate between active (GTP-bound) and inactive (GDP-bound) forms, which turn the downstream signaling on and off by association/dissociation with a subset of effector molecules. Three members of the family have been studied in detail: RhoA, Rac1 and Cdc42 [6]. In most cell types, RhoA stimulates stress fiber formation, Rac1 induces membrane ruffling and lamellipodia formation, and Cdc42 mediates filopodia formation [7-10]. Narrow-band UVB activates Rac1 signaling, resulting in increased dendrite formation, in B16 melanoma [11]. According to Ito et al., centaureidin inhibits dendrite outgrowth and methylophiopogonanone B induces dendrite retraction by increasing levels of Rho-GTP in melanocytes [12, 13]. Although several studies have shown changes in dendricity of melanocytes, it is still unknown whether changes in dendricity alleviate UV-induced hyperpigmentation.

Pyruvate, a three-carbon α-keto monocarboxylate, is the keystone metabolite in glycolysis and is mainly metabolized through the tricarboxylic acid (TCA) cycle. Elevated levels of

exogenous pyruvate promote mitochondrial oxidative phosphorylation for energy generation. Previous studies have demonstrated that aberrant serum pyruvate levels correlate with several diseases, including metabolic acidosis, sepsis, motor neuron disease, MELAS, and other disease. Treatment with hypertonic sodium pyruvate ameliorates hemorrhagic shock and ischemic-reperfusion injury [14-16].

In this study, we demonstrated that elevated extracellular sodium pyruvate inhibits melanogenesis depending on the rate of pyruvate uptake through H^+/monocarboxylate transporters (MCT). The α-MSH-induced morphological changes in melanocytes, such as dendrite outgrowth and branching, are reduced by treatment with sodium pyruvate. Pyruvate represses Rac1 GTPase activation in leading to inhibit dendrite elongation. We also studied the anti-melanogenic and dendrite extension inhibitory effects of pyruvate on alleviating the UV irradiation-induced hyperpigmentation in a reconstructed human pigmented skin equivalent (RHPE) model. These results show the activity of pyruvate as an effective molecule to prevent hyperpigmentation and help improve skin conditions such as evenness and translucency.

2. Materials and methods

2.1 Cell culture

The B16F10 cells were cultured in calcium free Dulbecco's Modified Eagle's Medium (DMEM) supplemented with 10 % fetal bovine serum (FBS), penicillin (400 units/mL), streptomycin (50 g/mL) and 0.01 mM of $CaCl_2$. Neonatal human epidermal melanocytes (NHEMs) were purchased from Lonza, and cultured in melanocyte growth medium-4 (MGM-4) media. Cells were maintained in a humidified 5 % CO_2 atmosphere, at 37 °C.

2.2. Measurement of melanin contents

Cells (2×10^5) were cultured in a 6-well plate for 24 h, and treated with 10 nM of α-MSH with or without 10 mM of pyruvic acid or sodium pyruvate. Thereafter, the cells were washed twice with phosphate-buffered saline (PBS) and harvested. Cells were lysed by incubating in 60 μl of 1N NaOH, at 80℃ for 30 min. The cell lysates were transferred to a 96-well plate, and measured at 405 nm. α-Cyano-4-hydroxycinnamic acid (Sigma-aldrich, USA) were treated 30 min before sodium pyruvate treatment.

2.3. Western blot analysis

All lysates were prepared in 5x lysis buffer. All cellular proteins were quantified using BCA protein assay kit (Pierce, USA), according to the manufacturer`s instructions. The samples were then separated by SDS-PAGE and transferred to a Nitrocellulose membrane (Invitrogen, USA). After blocking with 3% (w/v) BSA in TBST, the membranes were incubated overnight with specific primary antibodies. The anti-tyrosinase antibody (sc-7834), anti-TRP1 antibody (sc-10448) were purchased from Santa Cruz and anti-TRP2 antibody (74073) were purchased from Abcam. For protein detection, the membranes were incubated with HRP-conjugated secondary antibodies, and the signals were detected with Fusion FX 5 image system (Vilber Lourmat, France).

2.4. Measurement of intracellular pyruvate

The measurement was performed using Pyruvic acid assay kit (Megazyme, Ireland) according to the manufacturer`s recommendations, with minor modifications. Briefly, B16F10 cell (5×10^6) were lysed by 0.25 ml Tris/EDTA buffer (25 mM Tris, pH 8.0; 5 mM EDTA; 1% Triton X-100) and 20 μl of NADH was added for 2 min. The sample was mixed thoroughly and the

absorbance (A1) was recorded at 340 nm. Thereafter, 2 μl of D-LDH solution was added and the sample was incubated for 3 min. The absorbance (A2) at 340 nm was measured again. The change of absorbance at 340 nm (ΔA= A1 – A2) was used to calculate pyruvate concentration. The pyruvate content was normalized for total protein content.

2.5. Immunofluorescence staining

The primary melanocytes were fixed in cold methanol at -20℃ for 20 min and followed by permeabilization in 0.5% triton X-100 in PBS for 15 min. The primary antibodies were added overnight at 4℃, followed by incubation with appropriate secondary antibody for 1 h at room temperature. The images were captured with EVOS FL auto 2 (Thermo Fisher Scientific, USA) and post-processed using Image J program.

2.6. Pull-down assay of cellular GTP-Rho, Rac1 and Cdc42

The B16F10 cells (1×10^6 cells) were lysed in cold lysis buffer (50 mM Tris, pH 7.5, 10 mM $MgCl_2$, 0.2 M NaCl, 2% NP-40, 10% sucrose) on ice. The lysate was pre-cleared by incubation with glutathione beads. Either GST-Rhotekin (2 mg/ml) or GST-PBD (3 mg/ml) (both purchased from Cytoskeleton) was added to the cleared lysates in the binding buffer (50 mM Tris, pH 7.5, 60 mM $MgCl_2$, 80 mM NaCl, 1% NP-40, 1 mM NaF, 50 μM dithiothreitol), for 1 h at 4℃. The GTP-bound proteins were captured by incubation with glutathione beads. The beads were washed with binding buffer, and GTP-bound protein was eluted with 5X sample buffer. The samples were subjected to western blotting using anti-Rac1 antibody (Abcam, UK), anti-RhoA antibody, and anti-Cdc42 antibody (Santa Cruz biotechnology, USA).

2.7. Fontana-Masson staining

Reconstructed human pigmented epidermis model (Neoderm-ME, Melaskin) were purchased from Tego science Co (Seoul, Korea) and Biosolutions (Seoul, Korea). A solution of 1% Sodium pyruvate was applied topically on the surface of the reconstructed pigmented human epidermis model. After 7 days, 3D human skin-equivalent blocks were fixed with 10% neutral-buffered formalin and embedded in paraffin. The paraffin blocks (3 mm thickness) were sectioned and transferred onto slides. After deparaffinization, the sections were stained with the F/M staining kit from American Master Tech Scientific, Inc (Lodi, CA), according to the manufacturer`s instructions. After dehydrating and washing, the sections were observed at 400x magnification using a microscope (Thermo Fisher Scientific, USA). For quantitative analysis, pixels were selected in regions with melanin among entire area by determining the intensity in RGB (red, green and blue) channels with the Image J software.

2.8. Statistical analysis

Data are expressed as means ± SD (standard deviation) values, and Student`s t-test was used for statistical comparisons. A p-value < 0.05 was considered statistically significant (individual p-values are given in figure legends).

3. Results

3.1. The anti-melanogenic efficacy of pyruvate is altered by the activity of the pH-dependent MCT transporter.

Recently, Zhou *et al*. demonstrated that pyruvic acid/ethyl pyruvate inhibits melanogenesis in B16F10 murine melanoma. However, they could not find the anti-melanogenic activity of

sodium pyruvate, and the anti-melanogenic activity of pyruvic acid weakened upon neutralization with NaOH [17]. To determine whether the extracellular concentration of [H^+] ions modulates the efficacy of pyruvate on melanogenesis, we measured the melanin content by raising the pH from 6.5 (10 mM of pyruvic acid in medium) to 7.5 (10 mM of sodium pyruvate in medium). As shown in Fig. 1A, we found that as the pH of the medium containing pyruvic acid was increased by NaOH, the anti-melanogenic efficacy decreased, and at pH 7.5, sodium pyruvate had an inhibitory activity similar to pyruvic acid at pH 7.5. At pH condition 6.5 to 7.5 without pyruvate treatment, no inhibition of melanogenesis was observed (Supplementary Fig. 1A). Interestingly, Sodium pyruvate and pyruvic acid did not show exactly the same efficiency at the same pH and that efficacy of pyruvate varies depending on the type of dissociated salt (Supplementary Fig. 1B). Following treatment with sodium pyruvate at pH 7.5, the western blotting results showed that the expression of tyrosinase, TRP1 and TRP2 was significantly lower than the levels observed upon α-MSH induction without sodium pyruvate treatment (Fig. 1B). We also confirmed that sodium pyruvate treatment in NHEMs exhibited a decreased number of L-DOPA-stained-cells compared with untreated cells in a dose-dependent manner (Supplementary Fig. 1C). To evaluate the direct inhibition of tyrosinase activity under treatment with sodium pyruvate and pyruvic acid at same pH, we performed *in vitro* mushroom tyrosinase inhibitory assay at pH 7 buffering condition. We used lactate, which is another well-known monocarboxylate, as a positive control and the inhibitory effect of lactic acid on melanin synthesis was previously reported [18, 19]. Sodium pyruvate exerted a mushroom tyrosinase inhibitory effect (approximately 29% at 25 mM, and 36% at 50 mM of sodium pyruvate, and 17% at 25 mM, 50% at 50 mM of pyruvic acid) (Supplementary Fig. 1D).

Previous studies have shown that the transport of pyruvate across cell membranes is mediated by MCTs. According to Lin et al., the uptake of pyruvate by MCT1 or MCT2 is inhibited as the extracellular pH increases from 6.0 to 8.5 [18]. To study whether the pH-dependent inhibitory activity of pyruvate on melanogenesis was regulated by the MCT pumps, we measured the intracellular concentration of pyruvate at increasing extracellular pH from

6.5 to 7.5. The rate of pyruvate uptake decreased by more than 60 % when the pH of pyruvic acid containing medium was elevated from 6.5 to 7.5 and the rate of pyruvate transport in pyruvic acid-treated medium at pH 7.5 was similar to that of sodium pyruvate medium at pH 7.5. To investigate whether pyruvate uptake is necessary to inhibit melanin biosynthesis, we examined effect of α-cyano-4-hydroxycinnamic acid (CHCA), which is an MCT inhibitor, on the anti-melanogenic activity of pyruvic acid or sodium pyruvate treatment. As shown in Fig 1D, the treatment of sodium pyruvate with CHCA had less effect on the expression of tyrosinase, TRP1 and TRP2, than treatment without CHCA, however, CHCA alone had no anti-melanogenic effect (Fig. 1D, Supplementary Fig. 1E). These results indicate that sodium pyruvate also has an inhibitory effect on melanin content, depending on the intracellular pyruvate level caused by MCTs-mediated pyruvate uptake.

3.2. Sodium pyruvate regulates dendrite outgrowth of murine B16F10 cells and human primary melanocytes

Interestingly, the α-MSH-induced multiple arborizing dendrites and growth-cone-like morphology was inhibited and the length of dendrites was diminished in B16F10 cells, upon treatment with sodium pyruvate (Fig. 2A and Supplementary Fig. 2). To confirm the effect of sodium pyruvate on dendrite formation, we performed immunostaining with a TRP2 antibody using primary normal human epidermal melanocytes (NHEM) to evaluate the number and length of dendrite branches (Fig. 2B). Dendrites length was markedly inhibited under sodium pyruvate treatment in a dose-dependent manner (control, 100 μm; 1 mM pyruvate, 83.7 μm; 10 mM pyruvate, 71 μm), and the number of cells with more than 3 dendrite branches was decreased under sodium pyruvate treatment (control, 67.7%; 1 mM pyruvate, 52.6%; 10 mM pyruvate, 39.3%) (Fig. 2B). These results indicate that sodium pyruvate may be involved in dendrite formation. Therefore, in view of this result, we proceeded to investigate how sodium pyruvate functions in dendrite retraction.

3.3. Sodium pyruvate inhibits α-MSH-stimulated Rac1 activation

Small GTPases, such as Rac1, RhoA, and Cdc42 have been shown to regulate assembly and disassembly of actin reorganization and dendrite/branch formation in melanocytes [5, 20]. To assess their role in the dynamic cytoskeletal changes induced by sodium pyruvate, we performed a pull-down assay for Rho GTPase family members using B16F10 cells. The analysis revealed that GTP bound Rac1 protein was significantly decreased upon treatment with sodium pyruvate. The Cdc42-GTP and RhoA-GTP contents exhibited minor alterations following treatment with sodium pyruvate (Fig. 3). These results indicate that sodium pyruvate both suppresses Rac1 activation and dendrite outgrowth.

3.4. Pyruvate showed anti-melanogenic activity in the reconstructed human pigmented epidermis.

To extend this investigation to a physiological system, we examined the anti-melanogenic ability of sodium pyruvate in a pigmented skin equivalent, which was established by co-seeding melanocytes and keratinocytes and culturing it for 6 weeks at the air-liquid interface. For visualizing the melanin in the skin equivalent, Fontana-Mason (F&M) staining was performed. Under 1% sodium pyruvate treatment, in which the concentration did not induce tissue collapse (Supplementary Fig. 3), melanin content was decreased compared to PBS treatment in a dose-dependent manner (the ratio of melanin pixel/total area pixel (%); 1% of sodium pyruvate, 62% versus control; 0.1% treatment, 73% versus control; 0.01% treatment, 88% versus control and 4% hydroquinone as a positive control, 42% versus control) (Fig. 4A and B). Moreover, using F-M staining and immunostaining with anti-gp-100 antibody, we found that sodium pyruvate-treated tissue had clearly retracted dendrites compared to the control tissue (Fig. 4C). These results support the inhibitory efficacy of topical application of sodium

pyruvate in dendrite formation of melanocytes, leading to the promotion of depigmentation in the pigmented epidermis model.

3.5. Pyruvate treatment alleviates UV-induced hyperpigmentation

Next, to examine the effect of sodium pyruvate on UV-induced pigmentation, the skin equivalent was irradiated twice a week (25 J/cm^2 total UVA) and treated with or without sodium pyruvate on the stratum corneum. In Fig. 5A (left panel), sodium pyruvate-treated non-irradiated tissue appeared lighter than the control tissue. Under UV irradiation, the pigmented area was markedly increased compared to the non-irradiated tissue, whereas sodium pyruvate inhibited this pigmentation. From these results, we can conclude that sodium pyruvate treatment is significantly effective in reducing UV-induced hyperpigmentation.

4. **Discussion**

Exogenous pyruvate, which lies at the intersection of multiple metabolic pathways, has been implicated in embryogenesis, carcinogenesis, and differentiation, but most studies have focused on its role in metabolism and reactive oxygen species scavenging. This study revealed that extracellular pyruvate is absorbed into cells through the MCT transporter, preventing melanin synthesis and modulates both dendritic balance and Rac1 activity.

We found that pyruvate suppressed Rac1 activity in inhibiting the elongation of dendrite outgrowth, which may be in agreement with a report by Zhou et al. that pyruvic acid or ethyl pyruvate activated PI3K/Akt and, ERK signaling in melanocytes. The PI3K/Akt and MAPK pathways are implicated in not only melanogenesis but also in dendrite outgrowth. It is well documented that elevated p-ERK and p-Akt levels inhibit melanin synthesis by regulating

microphthalmia-associated transcription factor (MITF) and subsequent expression of tyrosinase, TRP1 and TRP2 [17, 21, 22]. In addition, ERK1/2 is involved in UVA-induced melanogenesis [23]. The p38 MAPK-MKK6 pathway increases melanocyte dendricity by activating Rho family GTPase [24]. Interestingly, early reports suggested that Rac1 and Cdc42 could act as downstream [25, 26] and upstream [27-29], of PI3Ks. In this study, in addition to the inhibition of melanin biogenesis by pyruvate, we identified an additional function of pyruvate inhibiting dendrite outgrowth. However, the involvement of the pyruvate-regulated Rac1 pathway in melanocyte dendrites and melanogenesis, has not yet been clearly elucidated. How altered metabolism integrates with genetic programs to regulate melanocyte function and fate is a key unresolved question. It would be interesting to further explore how pyruvate-induced alteration of metabolism and PI3K pathways interact to coordinate dendrite branching.

In this study, we also demonstrated that pyruvate plays a significant role in ameliorating UV-induced pigmentation. These findings were strongly supported by skin equivalent experiments, showing that topical treatment of pyruvate inhibited dendrite outgrowth of melanocytes and alleviated the hyperpigmentation responses after stimulation by UV.

Hence, we may conclude that pyruvate prevents the development of the initial stage of melanogenesis (conversion of tyrosine to melanin via a cascade of specific enzymes) to terminal differentiation (dendrites branching to neighboring keratinocytes). These anti-melanogenic features of pyruvate have potential for the development of strategies to prevent pigment-related disorders.

Our observation further extends the previously established role of the Rac1 pathway as a necessary mediator of UV response that regulates the induction of dendrite formation [27]. Metabolites or other energy sources are expected to drive similar results in regulating dendrite formation. Future investigations will help to uncover other details regarding the mechanism and the specific effectors involved in the regulation of dendrite elongation under metabolic

switching.

Conflict of interest

None

Acknowledgements

This work was supported by the Future Core Research Institute of LG Household and Health Care, Ltd.

Reference

[1] J. D'Orazio, S. Jarrett, A. Amaro-Ortiz, T. Scott, UV radiation and the skin, International journal of molecular sciences 14(6) (2013) 12222-48.
[2] K. Van Den Bossche, J.M. Naeyaert, J. Lambert, The quest for the mechanism of melanin transfer, Traffic (Copenhagen, Denmark) 7(7) (2006) 769-78.
[3] T.B. Fitzpatrick, M. Miyamoto, K. Ishikawa, The evolution of concepts of melanin biology, Archives of dermatology 96(3) (1967) 305-23.
[4] M. Hara, M. Yaar, B.A. Gilchrest, Endothelin-1 of keratinocyte origin is a mediator of melanocyte dendricity, The Journal of investigative dermatology 105(6) (1995) 744-8.
[5] G. Scott, Rac and rho: the story behind melanocyte dendrite formation, Pigment cell research 15(5) (2002) 322-30.
[6] K. Burridge, K. Wennerberg, Rho and Rac take center stage, Cell 116(2) (2004) 167-79.
[7] A.J. Ridley, A. Hall, The small GTP-binding protein rho regulates the assembly of focal adhesions and actin stress fibers in response to growth factors, Cell 70(3) (1992) 389-99.
[8] A.J. Ridley, A. Hall, Signal transduction pathways regulating Rho-mediated stress fibre formation: requirement for a tyrosine kinase, The EMBO journal 13(11) (1994) 2600-10.
[9] A.J. Ridley, H.F. Paterson, C.L. Johnston, D. Diekmann, A. Hall, The small GTP-binding protein rac regulates growth factor-induced membrane ruffling, Cell 70(3) (1992) 401-10.
[10] R. Kozma, S. Ahmed, A. Best, L. Lim, The Ras-related protein Cdc42Hs and bradykinin promote formation of peripheral actin microspikes and filopodia in Swiss 3T3 fibroblasts, Molecular and

cellular biology 15(4) (1995) 1942-52.
[11] W.Q. Wang, J.F. Wu, X.Q. Xiao, Q. Xiao, J. Wang, F.G. Zuo, Narrow-band UVB radiation promotes dendrite formation by activating Rac1 in B16 melanoma cells, Molecular and clinical oncology 1(5) (2013) 858-862.
[12] Y. Ito, A. Kanamaru, A. Tada, Centaureidin promotes dendrite retraction of melanocytes by activating Rho, Biochimica et biophysica acta 1760(3) (2006) 487-94.
[13] Y. Ito, A. Kanamaru, A. Tada, Effects of methylophiopogonanone B on melanosome transfer and dendrite retraction, Journal of dermatological science 42(1) (2006) 68-70.
[14] D.C. Gore, F. Jahoor, J.M. Hibbert, E.J. DeMaria, Lactic acidosis during sepsis is related to increased pyruvate production, not deficits in tissue oxygen availability, Annals of surgery 224(1) (1996) 97-102.
[15] F. Petrat, T. Ronn, H. de Groot, Protection by pyruvate infusion in a rat model of severe intestinal ischemia-reperfusion injury, The Journal of surgical research 167(2) (2011) e93-e101.
[16] P. Sharma, P.D. Mongan, Hypertonic sodium pyruvate solution is more effective than Ringer's ethyl pyruvate in the treatment of hemorrhagic shock, Shock (Augusta, Ga.) 33(5) (2010) 532-40.
[17] S. Zhou, K. Sakamoto, Pyruvic acid/ethyl pyruvate inhibits melanogenesis in B16F10 melanoma cells through PI3K/AKT, GSK3beta, and ROS-ERK signaling pathways, 24(1) (2019) 60-69.
[18] R.Y. Lin, J.C. Vera, R.S. Chaganti, D.W. Golde, Human monocarboxylate transporter 2 (MCT2) is a high affinity pyruvate transporter, The Journal of biological chemistry 273(44) (1998) 28959-65.
[19] A. Usuki, A. Ohashi, H. Sato, Y. Ochiai, M. Ichihashi, Y. Funasaka, The inhibitory effect of glycolic acid and lactic acid on melanin synthesis in melanoma cells, Experimental dermatology 12 Suppl 2 (2003) 43-50.
[20] A. Hall, Rho GTPases and the control of cell behaviour, Biochemical Society transactions 33(Pt 5) (2005) 891-5.
[21] J.H. Kim, S.H. Baek, D.H. Kim, T.Y. Choi, T.J. Yoon, J.S. Hwang, M.R. Kim, H.J. Kwon, C.H. Lee, Downregulation of melanin synthesis by haginin A and its application to in vivo lightening model, The Journal of investigative dermatology 128(5) (2008) 1227-35.
[22] H.J. Kim, I.S. Kim, Y. Dong, I.S. Lee, J.S. Kim, J.S. Kim, J.T. Woo, B.Y. Cha, Melanogenesis-inducing effect of cirsimaritin through increases in microphthalmia-associated transcription factor and tyrosinase expression, International journal of molecular sciences 16(4) (2015) 8772-88.
[23] H. Yanase, H. Ando, M. Horikawa, M. Watanabe, T. Mori, N. Matsuda, Possible involvement of ERK 1/2 in UVA-induced melanogenesis in cultured normal human epidermal melanocytes, Pigment cell research 14(2) (2001) 103-9.
[24] M.Y. Kim, T.Y. Choi, J.H. Kim, J.H. Lee, J.G. Kim, K.C. Sohn, K.S. Yoon, C.D. Kim, J.H. Lee, T.J. Yoon, MKK6 increases the melanocyte dendricity through the regulation of Rho family GTPases, Journal of dermatological science 60(2) (2010) 114-9.
[25] K. Reif, C.D. Nobes, G. Thomas, A. Hall, D.A. Cantrell, Phosphatidylinositol 3-kinase signals activate a selective subset of Rac/Rho-dependent effector pathways, Current biology : CB 6(11) (1996) 1445-55.

[26] S. Sarner, R. Kozma, S. Ahmed, L. Lim, Phosphatidylinositol 3-kinase, Cdc42, and Rac1 act downstream of Ras in integrin-dependent neurite outgrowth in N1E-115 neuroblastoma cells, Molecular and cellular biology 20(1) (2000) 158-72.
[27] G.A. Scott, L. Cassidy, Rac1 mediates dendrite formation in response to melanocyte stimulating hormone and ultraviolet light in a murine melanoma model, The Journal of investigative dermatology 111(2) (1998) 243-50.
[28] A. Bonni, A. Brunet, A.E. West, S.R. Datta, M.A. Takasu, M.E. Greenberg, Cell survival promoted by the Ras-MAPK signaling pathway by transcription-dependent and -independent mechanisms, Science (New York, N.Y.) 286(5443) (1999) 1358-62.
[29] C. Tournier, P. Hess, D.D. Yang, J. Xu, T.K. Turner, A. Nimnual, D. Bar-Sagi, S.N. Jones, R.A. Flavell, R.J. Davis, Requirement of JNK for stress-induced activation of the cytochrome c-mediated death pathway, Science (New York, N.Y.) 288(5467) (2000) 870-4.

Figure 1

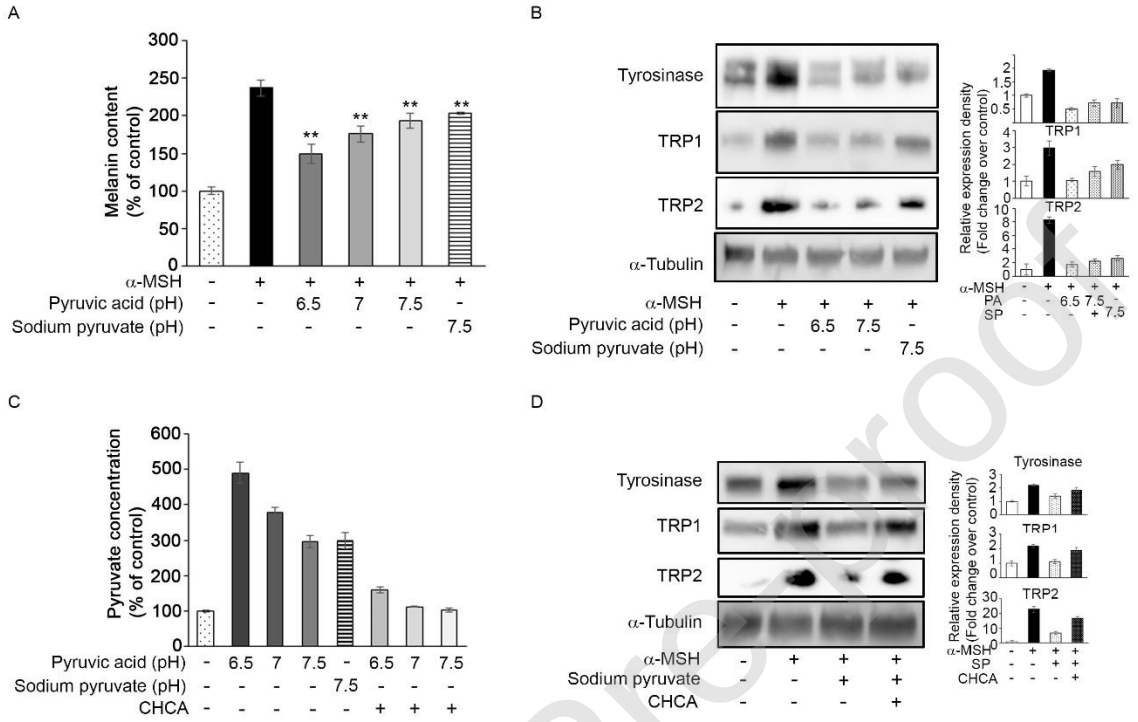

Fig. 1. The depigmentation efficacy of sodium pyruvate in a-melanocyte-stimulating hormone (α-MSH)-stimulated B16F10 murine melanoma cells. (A, B) Effect of pyruvic acid and sodium pyruvate on intracellular melanin in α-MSH-stimulated cells. B16F10 cells were treated with

10 mM of pyruvate in the presence of α-MSH 10 nM for 48 h at indicated pH. (A) Cell lysates were estimated by absorbance at 405 nm. The melanin contents were normalized for total protein contents. ** $p < 0.01$ versus the α-MSH treatment control (B) Protein levels present in the cell lysates were analyzed by western blot for Tyrosinase, TRP1, TRP2 and α-tubulin (loading control). Pyruvic acid treatment at pH 6.5 affect more to reduce these melanogenic enzymes. (C) Cells were treated with the indicated pH of pyruvic acid and sodium pyruvate in presence or absence of 500 μM CHCA. (D) Cells were treated with or without CHCA for 30 min. After treatment with α-MSH or sodium pyruvate for 48 h, the cell lysates were prepared and analyzed by western blotting, using indicated antibodies. Densitometric data are presented as the means ± SD of three independent experiments.

Figure 2

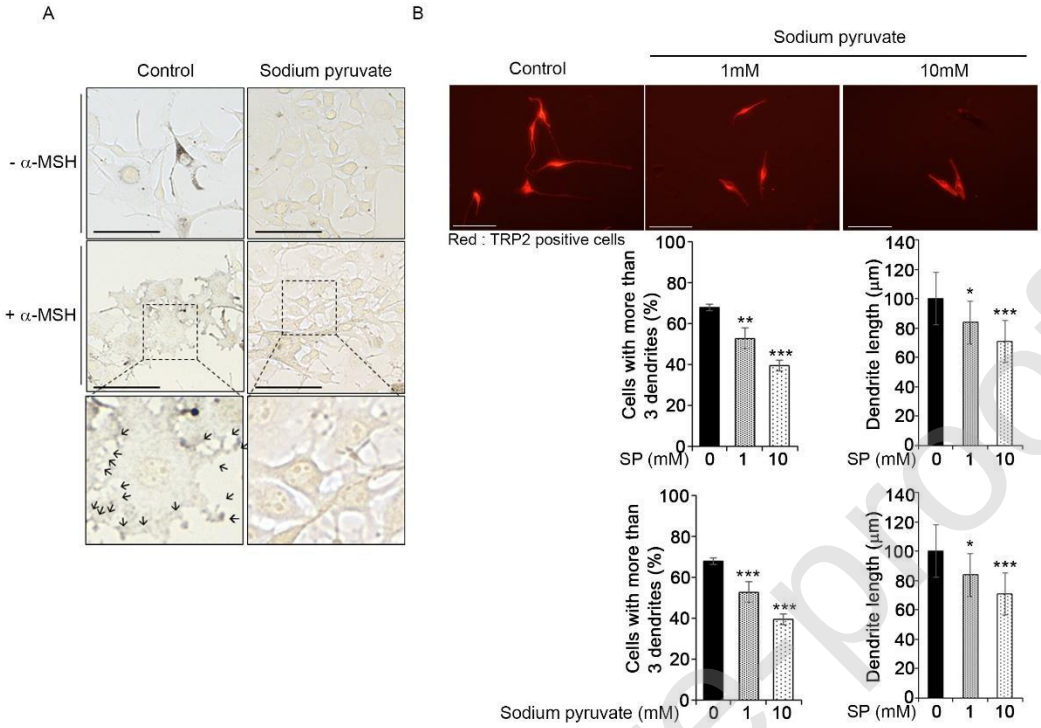

Fig. 2. The inhibitory effect of pyruvate on dendrite branching and size of melanocyte. (A) B16F10 cells were stimulated with 10 mM sodium pyruvate in presence or absence of α-MSH (10 nM) for 48 h. Dendrite formation were observed using microscopy. Scale bar: 100 μm. (B) Human primary melanocytes (NHEM) were treated with 1mM and 10mM of sodium pyruvate

during 48 h. For immunostaining, we stained melanocytes using TRP2 antibody (red color). Scale bar: 100 μm (upper). The graph shows the statistical results for reducing effect of pyruvate on the number of cells with more than 3 dendrite branches and size of each TRP2-positive cells. More than 40 cells were counted. *$p < 0.05$, **$p < 0.01$, ***$p < 0.001$ versus control. SP, sodium pyruvate.

Figure 3

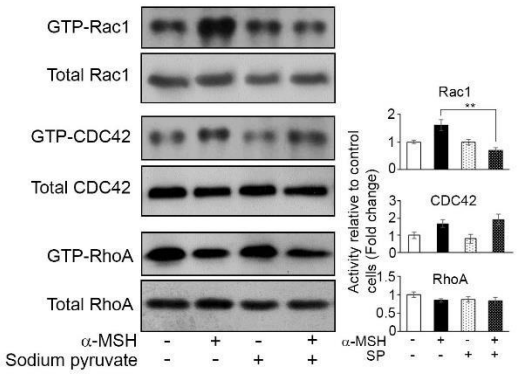

Fig. 3. Pull-down assay for small GTPase in pyruvate-treated melanocytes. NHEM were treated with (+) or without (-) 10 mM pyruvate, and GTP-bound Rac1, Cdc42 and RhoA were isolated by affinity purification. The pull-down precifitates and whole cell lysates were western

blotting using indicated antibodies. Values are expressed as means ± SD of at least three determinations. **$p < 0.01$ versus α-MSH treated control.

Figure 4

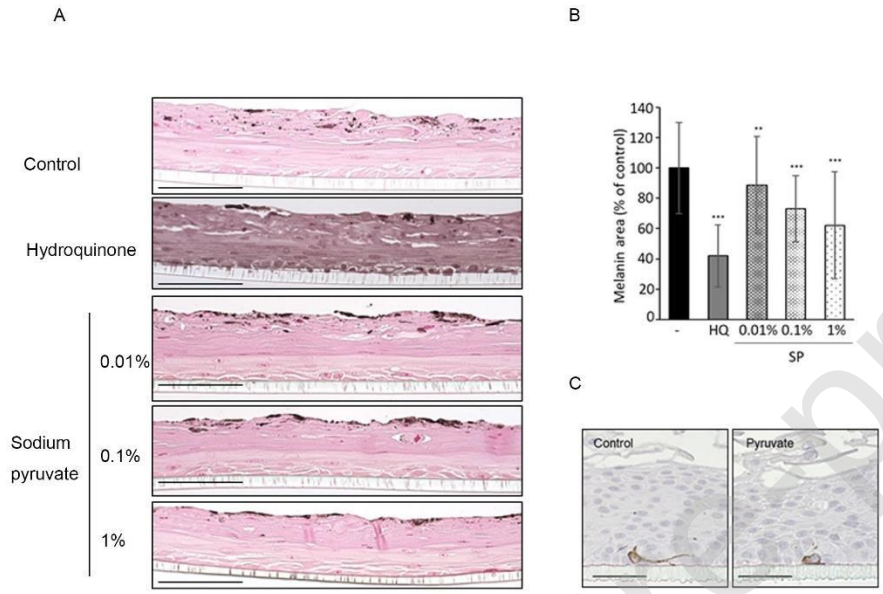

Fig. 4. Sodium pyruvate had an anti-melanogenic effect on skin equivalent (A, B, C) Neoderm-ME was pre-incubated for 24 h, then treated with (A) 1% (w/w, about 110mM), 0.1% (w/w, about 11mM) and 0.01% (w/w, about 1.1mM) of sodium pyruvate or 4% hydroquinone on stratum corneum every three days for 6 days. (A) Melanin pigmentation was observed upon Fontana-Masson (FM) staining. Scale bar: 100 μm. (B) The melanin contents was expressed as the percentage of melanin surface per epidermis surface compared to PBS treated control, $^{**}p < 0.01$, $^{***}p < 0.001$ versus untreated control. SP, sodium pyruvate. HQ, hydroquinone. (C) The morphology of melanocytes was visualized by immunohistochemical analysis using gp-100 antibody.

Figure 5

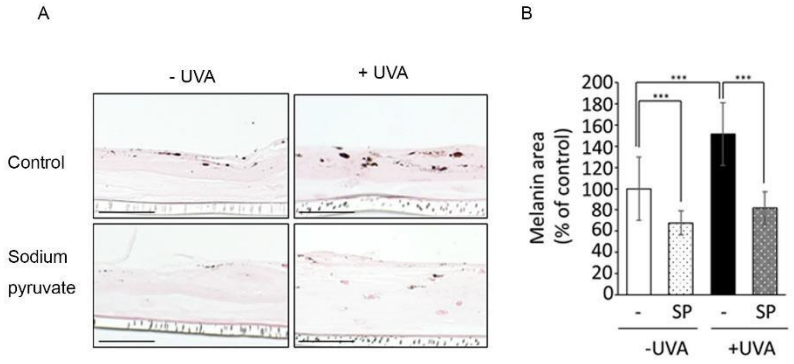

Fig. 5. Influence of pyruvate on UVA-induced pigmentation in reconstructed epidermis. (A, B) Reconstructed epidermis was irradiated with UVA (25 J/cm^2) 2 times in a week and treated with or without 10 mM sodium pyruvate on stratum corneum. (A) Melanin pigmentation was observed upon Fontana-Masson (FM) staining. Scale bar: 50 μm. (B) The melanin contents

was expressed as the percentage of melanin surface per epidermis surface, ***$p < 0.001$. SP, sodium pyruvate.